



RESEARCH ARTICLE

VORTEX DIPOLE EXCITATIONS IN TRAPPED BOSE-EINSTEIN CONDENSATE.

Qingli Zhu.

Department of information engineering, nanjing normal university taizhou college, taizhou 225300, china.

Manuscript Info

Manuscript History

Received: 10 November 2017

Final Accepted: 12 December 2017

Published: January 2018

Key words:-

vortex excitations, Gaussian obstacle potential, Bose-Einstein condensate, spin-orbit coupling.

Abstract

We numerically study dynamical creation of vortex excitations in Bose-Einstein condensates (BECs) within the framework of mean-field theory using dissipative Gross-pitaevskii equation. Vortex dipoles and soliton pairs are found to be created after two Gaussian obstacle potentials collide head on. Furthermore, we examine the mechanism of vortex excitation in a highly oblate spin-orbit coupling BEC. It is found that the symmetry of vortex dipoles is destroyed and the structure is quite different from that without spin-orbit coupling. The critical velocity for vortex-antivortex pair nucleation is heavily influenced by the strength of spin-orbit coupling.

Copy Right, IJAR, 2018,. All rights reserved.

Introduction:-

Since the vortex dipoles have been directly observed in a pancake-shaped condensate by forcing superfluid flow around a repulsive Gaussian obstacle potential(GOP)[1-2]. A variety of theoretical and experimental studies have been made on a scalar BEC, such as vortex dipoles induced in oscillating potential and at finite temperature[3-4]. Using two blue-detuned laser beams as "tweezers", one can pin and manipulate vortices on demand experimentally[5-6]. Recent progress in a toroidal geometry has opened a new prospect to study the superfluidity and vortex excitation[7-9]. Due to the progress in the field of ultracold atoms and the realization of synthetic non-Abelian gauge field, the SO coupling with bosons have received increasing attention theoretically[10]. The SO coupled condensates not only support various density profiles such as plan wave or striped wave in spin-1/2 condensate but also some elementary excitations such as vortex and skyrmion[11-13].

In this paper, we focus on the dynamical problem of a moving obstacle potential in an harmonic trap BEC. Despite there exist a lot of significant experimental and theoretical advances in this topic, the vortex excitations and dynamics are not associated for two obstacle colliding head on. Furthermore, motivated by the latest research on the dynamics of a moving obstacle in a uniform system of SO coupling BEC[14], we investigate the SO coupling effect on the nucleation and dynamics of vortices in an harmonic trap. We find that the SO coupling is favorable for vortices nucleation.

Model:-

We consider a single BEC described by the macroscopic wave function $\psi(\vec{r}, t)$. In the mean-field framework, the dynamics of a system with N weakly identical atoms close to thermo-dynamic equilibrium and subject to weak dissipation can be described by the dissipative Gross-pitaevskii(GP) equation[15]:

Corresponding Author:-Qingli Zhu.

Address:-Department of information engineering, nanjing normal university taizhou college, taizhou 225300, china.

$$(i - \gamma)\hbar\partial_t\psi(\vec{r}, t) = \left[\frac{\hbar^2\nabla^2}{-2m} + V(\vec{r}) + g|\psi(\vec{r}, t)|^2 \right] \psi(\vec{r}, t), \quad (1)$$

where $V(\vec{r}) = \frac{1}{2}m(\omega_x^2x^2 + \omega_y^2y^2 + \omega_z^2z^2)$ is the axially symmetric harmonic trap potential. $\omega_x = \omega_y = \omega_t$ is the radial trap potential frequency and ω_z presents the axial trap potential frequency. We focus in this paper on a pancake-shaped situation with $\omega_z \gg \omega_t$. In this extreme limit, the axial dimension is sufficiently thin that the motion along z direction can be neglected and atoms can move only within the xy plane. The wave function of BEC $\psi(\vec{r}, t)$ is normalized according to $\int d\vec{r}\psi^*(\vec{r}, t)\psi(\vec{r}, t) = N$. The last term in equation is the atom-atom contact

interaction which characterized by $g = \frac{4\pi\hbar^2a_s}{m}$ with a_s the s-wave scattering length and m the atom mass. We have neglected the chemical potential by a constant without affecting the dynamics. The parameter γ in GP equation is a dimensionless, phenomenological, damping constant which is always introduced to fit experiment. The dissipative GP equation has been extensively employed to study the dynamics of systems in the presence of thermally induced dissipation[16-18]. In present work, we neglect the possible dependence of γ on the position and temperature and assume it to be a constant.

In actual computation, we discrete the xy plane into a square lattice points. The space scale is much larger than the TF radius of the condensate. a is assumed to be the lattice constant whose value must be much less than the characteristic length $l = \frac{\hbar}{m\omega_t}$ of the axial harmonic oscillator so that the dynamics are independent of the grid. For

the time evolution forth-order Runge-kutta method is used at each time step. The central-difference formula is used mainly to calculate the diffusion term (kinetic term). Introducing dimensionless $\psi(i, j)$ in the GP equations, by substituting $\psi(\vec{r}, t)$ with $\frac{1}{\sqrt{a^2a_z}}\psi(i, j, t)$, where $a_z = \frac{\hbar}{m\omega_z}$ is the characteristic length of longitudinal harmonic

oscillator, we will thus obtain the following lattice-version of the GP equations:

$$(i - \gamma)\hbar\partial_t\psi(i, j, t) = \{ \tau[(\psi(i+, j) + \psi(i-, j) + \psi(i, j+1) + \psi(i, j-1) - 4\psi(i, j))] + [V(i^2 + j^2) + g|\psi(i, j)|^2] \psi(i, j) \} \quad (2)$$

where $\tau = \frac{\hbar^2}{2ma^2}$, $V = \frac{1}{2}m\omega_t^2a^2$, $g = \frac{4\pi\hbar^2a_s}{ma^2a_z}$. Now all the parameters τ, V, g and $\frac{\hbar}{\tau}$ have the scale of

energy. It is convenient to introduce dimensionless parameters $V' = \frac{V}{\tau}$, $g' = \frac{g}{\tau}$, $t' = \frac{t}{\hbar/\tau}$, measured in unit of τ . Finally the dimensionless GP equations can be expressed as

$$(i - \gamma)\frac{[\psi(i, j, t' + dt') - \psi(i, j, t')]}{dt'} = \{ [(\psi(i+, j) + \psi(i-, j) + \psi(i, j+1) + \psi(i, j-1) - 4\psi(i, j))] + [V'(i^2 + j^2) + g'|\psi(i, j)|^2] \psi(i, j) \} \quad (3)$$

The parameters in the above equations are all dimensionless and they are actually only dependent of $\frac{a}{l}$ and $\frac{a_s}{a_z}$. A

straightforward calculation leads to the following expressions of $V' = (\frac{a}{l})^4$ and $g' = 4\pi\frac{a_s}{a_z}$. Note that g' is essentially independent of the artificial lattice constant a .

We based our simulation on a condensate of $N = 1.0 \times 10^5$ atoms in a trap potential. Assuming the system consists of ^{87}Rb atoms, we have $m \approx 87m_p$ with m_p the mass of proton. The trap frequency is chosen to be $\omega_t = 2\pi \times 10\text{s}^{-1}$ and $\omega_z = 2\pi \times 100\text{s}^{-1}$, then l is estimated to be about $3.4\ \mu\text{m}$ and $\frac{\hbar}{\tau} = 1.27\text{ms}$. The square lattice we study is a 200×200 system and $(\frac{a}{l})^2 = 0.008$. This means the system has a size of about $60\ \mu\text{m} \times 60\ \mu\text{m}$ and $\frac{\hbar\omega_t}{\tau} = 2(\frac{a}{l})^2 = 0.016$. Therefore, we have $V' = 0.000064$. In addition, to guarantee both the convergence and efficiency of iteration of the GP equations, dt' is chosen to be between 0.0001 and 0.01 in numerical calculations. In the following, γ is set to be $\gamma = 0.0015$. We find our results do not depend qualitatively on the specific value of γ in the range from $\gamma = 0.001$ to $\gamma = 0.01$. The dissipative parameter determines the relaxation time of the vortices: the greater γ is, the less time it takes.

Results and discussion:-

1、two obstacle collide head on

In this section, we investigate numerically the dynamical behaviors of vortex dipoles excited by two uniformly moving Gaussian obstacle potentials (GOPs) when they collide head-on. To begin with, we first consider the situation where one GOP move in x direction. After getting the stationary solution using imaginary method only in the presence of a harmonic trapping potential, an obstacle potential is introduced and is fixed at one point until the condensate structure stable. This procedure avoids appearance of phase singularity trapped by the obstacle potential.

A single GOP moving through the condensate can be described as: $V_{\text{GOP}} = V_0 \exp[\frac{(x-x_0)^2 + y^2}{d^2}]$, where d is the width and V_0 is the amplitude of the obstacle potential maxima located at $(x(t), 0)$. In our numerical computation,

we choose $d = 0.8l$ and $V_0 = 8\tau$. For the condensate center density n_0 , the sound velocity $v_s = \sqrt{\frac{n_0 g}{m}}$. Consider an obstacle with gradually increasing velocity, on reaching the critical velocity, periodic vortex shedding starts. Then the critical velocity is determined. In our simulation is about $370\ \mu\text{m/s}$, which is about $0.6 v_s$. When the speed is in the range of $370\ \mu\text{m/s} < v < 450\ \mu\text{m/s}$, a vortex-antivortex pair can be nucleated.

Now, we turn to consider the collision of two GOPs. At initial time, two GOPs are displaced away from the condensate center for a equal distance. We set that two GOP are located at $(-4.4l, 0)$ and $(4.4l, 0)$ respectively. After the condensate in a static structure, two GOPs start to move along the x and $-x$ direction at a constant velocity $v = 405\ \mu\text{m/s}$. It should be pointed out that the intensity V_0 keeps constant until GOPs reaching the condensate edge and suddenly disappear.

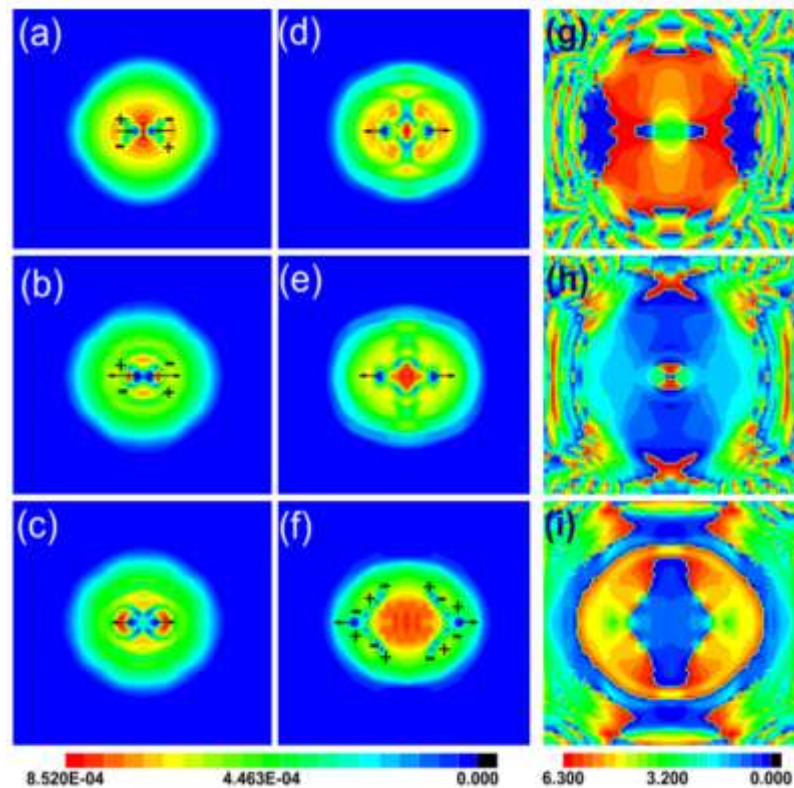


Fig.1 (color on line) The left and middle panels are the density profiles at (a) $t=31.75$ ms, (b) $t=41.275$ ms, (c) $t=47.625$ ms, (d) $t=53.975$ ms, (e) $t=60.32$ ms, (f) $t=69.85$ ms. The right panel (g)-(i) are the corresponding phase profiles of (a), (b), and (f) respectively. The symbol $+$ ($-$) denotes a vortex with counterclockwise (clockwise). Black arrows indicate the motion direction of potentials

Soon after the movement of two GOPs, two vortex dipoles are nucleated symmetrically about x and y axis behind the GOPs with opposite topological charge as shown in Fig.1(a). In the process of collision of two potentials, we do not find any excitation. But as two potentials separate from each other after collision, the impulses push the two vortex dipoles to pass through the potentials and move towards the lower density regimes left by two GOPs. The vortices and anti-vortices start to converge and form new structure after they met as shown in Fig.1(d). This structure is not stable and soon decays into vortex dipoles in Fig.1(e). When the two GOP near the edge of condensate, six pairs of vortex dipoles are nucleated symmetrically. Their density and phase profiles are shown in Fig.1(f) and Fig.1(i). In a word, the collision of two Gaussian repulsive potentials leads to the nucleation of new vortex dipoles.

Now, we focus on the dynamical decay of these vortex anti-vortex pairs. Fig.2 shows the density profiles of vortex dipoles in the temporal evolution process. In order to identify every vortex and antivortex, we mark them with number 1-12. First, two vortex and antivortex pairs 1-2 and 3-4 nucleated behind the potentials move away from the condensate. When arriving at the edge, they divorce and move in opposite directions along the surface. On the contrary, vortex 5 and 7 would converge anti-vortex 6 and 8 move towards the condensate center and eventually annihilate in a circle form, as shown in Fig.2(f). Subsequently, vortex 9 and 11 would converge anti-vortex 12 and 10 move towards each other until they meet in the condensate center. After this, a pair of solitons gets generated. We can observe clearly the propagation of two solitons along opposite direction in Fig.2(i). After reaching condensate edge, the two solitons collapse into two vortex pairs. So far, all the vortices and anti-vortices are ejected out of the condensate. The condensate gets stable gradually.

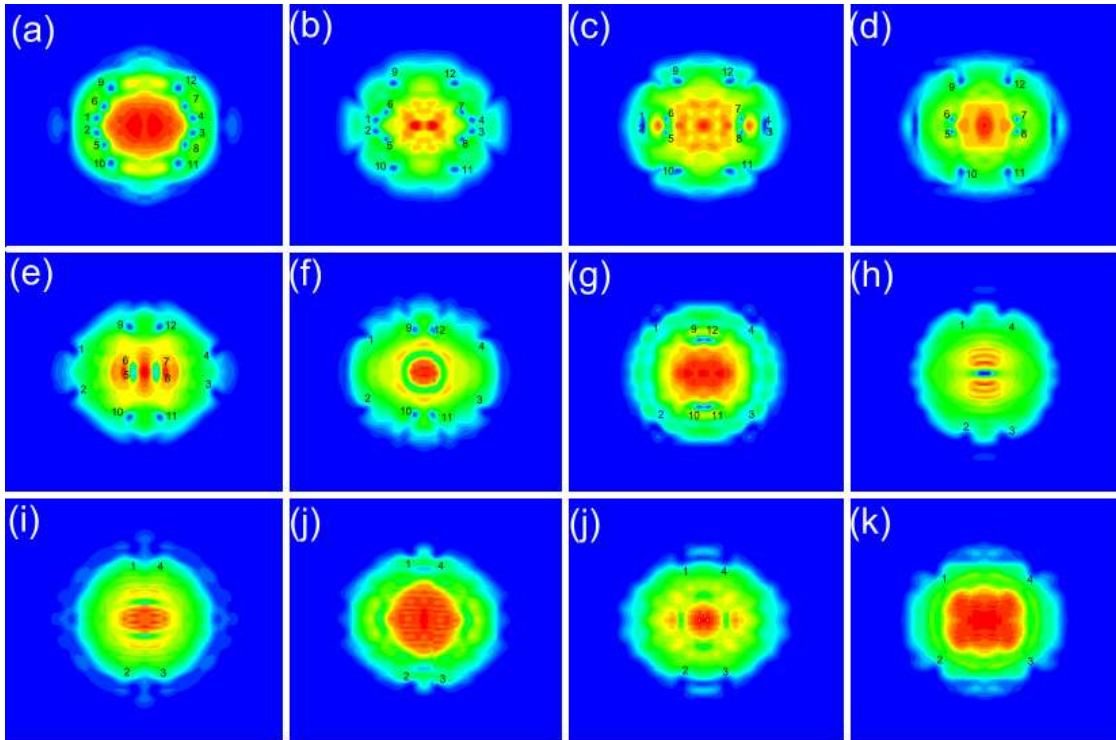


FIG.2 (color online) Density profiles in the dynamical evolution of vortices and anti-vortices at different time. From (a) to (l), the time is 88.90 ms, 101.60 ms, 114.30 ms, 120.65 ms, 139.70ms, 152.40ms, 165.10ms, 184.15ms, 190.50ms, 203.20ms, 209.55ms, 222.25ms. The odd numbers (1,3,5,7,9,11) denote anti-vortices while the even numbers (2,4,6,8,10) denote vortices.

2、vortex excitations under Spin-orbit coupling

To begin with, we consider a system of Rashba spin-orbit coupling on spin-1/2 BECs condensates confined in a harmonic trap. The Hamiltonian can be written $\hat{H} = \hat{H}_0 + \hat{H}_{\text{int}}$, where

$$\hat{H}_0 = \int d^2r \hat{\psi}^\dagger(\vec{r}, t) \left[\frac{\hbar^2 \nabla^2}{2m} + V(\vec{r}) + v_{so} \right] \hat{\psi}(\vec{r}, t) \text{ and } \hat{H}_{\text{int}} = \int d^2r [g_1 \hat{n}_\uparrow^2 + g_2 \hat{n}_\downarrow^2 + 2g_{12} \hat{n}_\uparrow \hat{n}_\downarrow].$$

Here, m is the atom mass and assumed to be equal for two components, $\hat{\psi}(\vec{r}, t) = [\hat{\psi}_\uparrow(\vec{r}, t), \hat{\psi}_\downarrow(\vec{r}, t)]^T$ denotes the spinor field operators and $\hat{n}_\uparrow = \hat{\psi}_\uparrow^\dagger \hat{\psi}_\uparrow$, $\hat{n}_\downarrow = \hat{\psi}_\downarrow^\dagger \hat{\psi}_\downarrow$. g_1, g_2 denote the self-interaction of component (intracomponent coupling) and are always taken to be equal $g_1 = g_2 = g$. g_{12} measures the effect of interaction between the two components (intercomponent coupling). For Rashba spin-orbit coupling, $V_{\text{soc}} = \frac{-i\hbar k_0 \nabla}{m} (\partial_x \sigma_x + \partial_y \sigma_y)$ with σ_x, σ_y being the Pauli matrices and k_0 characterizing the SO coupling strength that is assumed to be equal in both x and y directions.

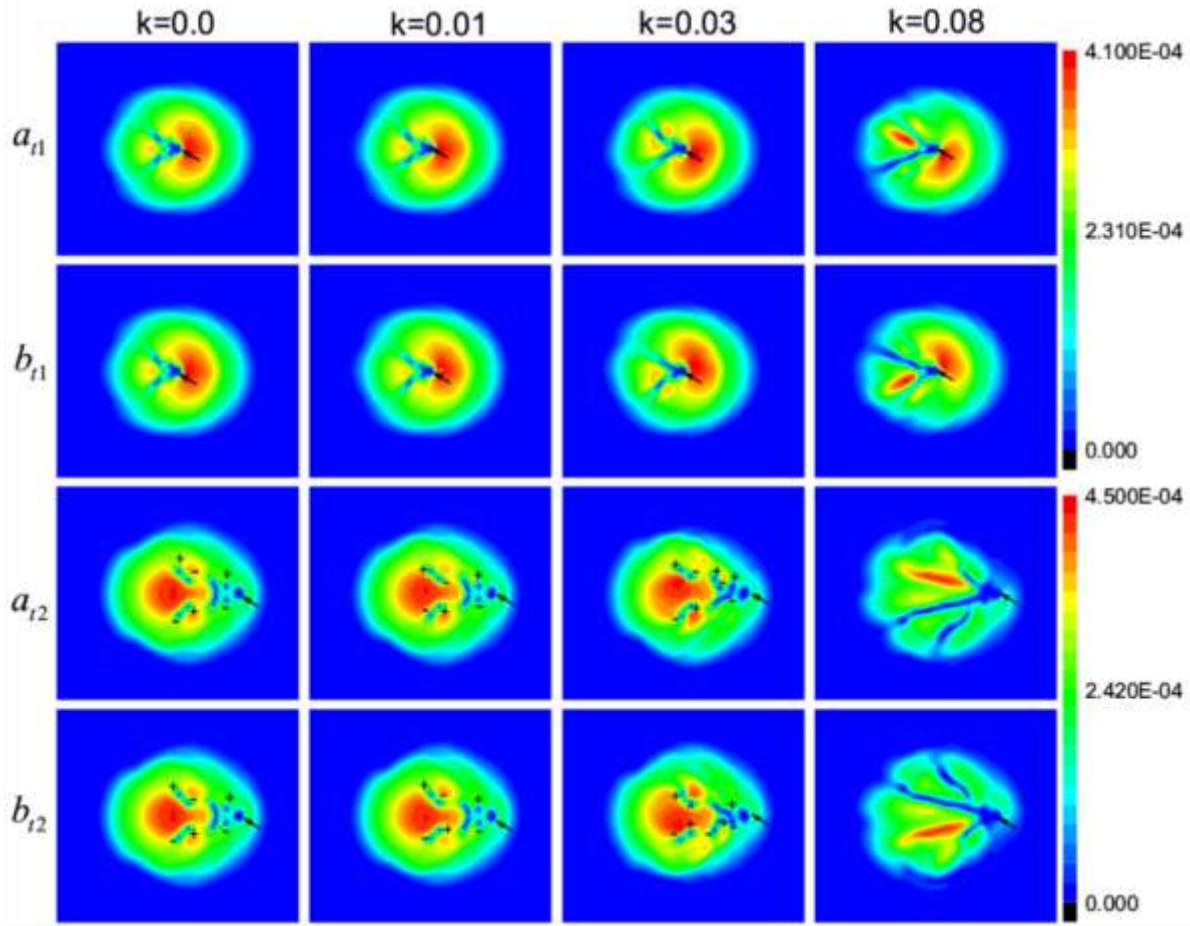


Fig.3 (color online). The density profiles of spin-1/2 two components with the uniform moving GOP when considering the influence of SO coupling for $k=0, k=0.01, k=0.03, k=0.08$ from left to right column. Two components here are represented by a and b. The first and second panels denote the situation when the GOP move near the condensates center at $t_1 = 31.75\text{ms}$. The third and the last panels denote the situation when the GOP near the condensates edge at $t_2 = 63.5\text{ms}$.

In this section, we mainly discuss the influence of SO coupling strength on the vortex nucleation when a GOP uniformly moving through the condensate. Before doing so, it is useful to study the properties of such a system without SO coupling. If $g_{12} < g$ the ground states of BEC are plan waves and the two spin components having the same ground state structure[11], the dynamical generation and evolution of vortex dipoles also takes on the same density distribution keep axial symmetry along x direction, as shown in Fig.3. In the presence of SO coupling, we first discuss the situation when the SO coupling strength is weak. In Fig.3, the GOP moves with the same speed 530um/s in all cases. We find that when SO coupling strength k is up to 0.03, the property of the density profiles start to different from each other. According to the results of Fig.3 we can see that the axial symmetry is broken in each component but maintained in the system if two components is considered as a whole. Furthermore, the vortex core in each component is occupied by the other component. This structure can therefore be regarded as a pair of half-quantum vortices. With the increase of SO coupling strength, more vortex dipoles would be nucleated and the symmetry along the x-axis would be destroyed for the system. The critical speed for $k=0.25$ is 130 um/s , which is far less than $v_c = 370\text{ um/s}$ mentioned above, meaning that the SO coupling effect is of benefit to the creation of the vortex dipole. The critical velocities for vortex dipole nucleation at different SO coupling strength are calculated and shown in Fig.4.

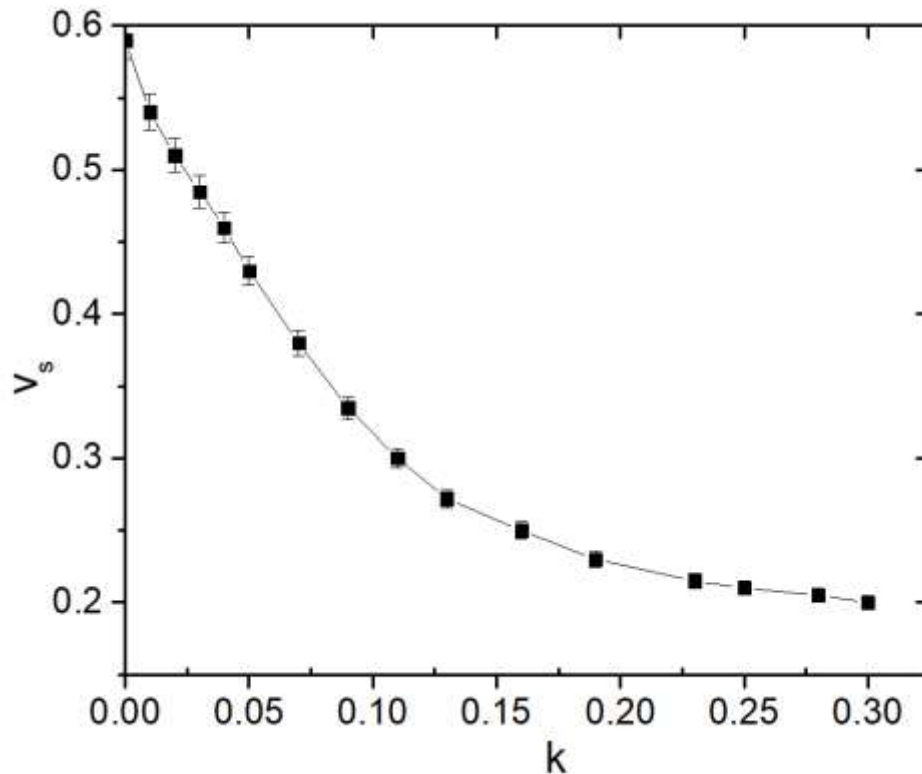


Fig.4:- The dependence of critical velocity on the SO coupling strength.

Conclusion:-

We have performed numerical calculations of the quasi-two-dimensional GP equation to investigate the creation and dynamical evolution of vortices in a harmonic trap potential. As two GOPs move and collide head on, we find extra vortex dipoles and a pair of solitons are nucleated symmetrically after the two GOPs separating from each other which enrich the phase profiles of vortex excitations. when a trapped SO coupling BEC is in a plane-wave phase, it is favorable for vortex creation under the influence of SO coupling effect. The velocity of a vortex-antivortex is much smaller than that without SO coupling.

Reference:-

1. T. W. Neely, E. C. Samson, A. S. Bradley, M. J. Davis and B. P. Anderson, Observation of vortex dipoles in an oblate Bose-Einstein condensate. *Phys. Rev. Lett.* 104, 160401 (2010)
2. D. V. Freilich, D. M. Bianchi, A. M. Kaufman, T. K. Langin and D. S. Hall, Real-Time dynamics of single vortex
3. lines and vortex dipoles in a Bose-Einstein condensate. *Science*. 329, 1182 (2010)
4. Fujimoto K. and Tsubota M. Nonlinear dynamics in a trapped atomic Bose-Einstein condensate induced by an oscillating Gaussian potential. *Phys. Rev. A* , 83 (2011) 053609.
5. S. Gautam, Arko Roy, and Subroto Mukerjee. Finite-temperature dynamics of vortices in Bose-Einstein condensates. *Phys. Rev. A*. 89, 013612 (2014)
6. Gertjerenken B., Kevrekidis P. G., Carretero-Gonzalez R. and Anderson B. P., Deterministic creation, pinning, and manipulation of quantized vortices in a Bose-Einstein condensate. *Phys. Rev. A*, 93 (2016) 023604
7. Wright K. C., Blakestad R. B., Lobb C. J., Phillips W. D. and Campbell G. K., Driving phase slips in a superfluid atom circuit with a rotating weak link. *Phys. Rev. Lett.*, 110 (2013) 025302
8. Eckel S., Jendrzejewski F., Kumar A., Lobb C. J. and Campbell G. K., Interferometric measurement of the current-phase relationship of a superfluid weak link. *Phys. Rev. X* , 4 (2014) 031052
9. Yakimenko A. I., Isaieva K. O., Vilchinskii S. I. and Ostrovskaya E. A., Vortex excitation in a stirred toroidal Bose-Einstein condensate. *Phys. Rev. A* , 91 (2015) 023607
10. Abad M, Deterministic creation, pinning, and manipulation of quantized vortices in a Bose-Einstein condensate. *Phys. Rev. A* , 93 (2016) 023603

11. Y. J. Lin, K. Jimenez-Garcia, and I. B. Spielman, Spin-orbit-coupled Bose-Einstein condensates, *Nature* (London). 471, 83 (2011).
12. C. J. Wang, C. Gao, C.-M. Jian, and H. Zhai, Spin-Orbit Coupled Spinor Bose-Einstein Condensates. *Phys. Rev. Lett.* 105, 160403 (2010).
13. T. L. Ho and S. Zhang, Bose-Einstein Condensates with Spin-Orbit Interaction. *Phys. Rev. Lett.* 107, 150403 (2011).
14. C. F. Liu, and W. M. Liu, Spin-orbit-coupling-induced half-skyrmion excitations in rotating and rapidly quenched spin-1 Bose-Einstein condensates. *Phys. Rev. A.* 86, 033602 (2012).
15. Kato M., Zhang X. F. and Saito H., Moving obstacle potential in a spin-orbit-coupled Bose-Einstein condensate. *Phys. Rev. A*, 96 (2017) 033613
16. S. Choi, S. A. Morgan, and K. Burnett, Phenomenological damping in trapped atomic Bose-Einstein condensates. *Phys. Rev. A.* 57, 4057 (1998).
17. Yakimenko A. I., Bidasyuk Y. M., Weyrauch M., Kuriatnikov Y. I. and Vilchinskii S. I., Vortices in a toroidal Bose-Einstein condensate with a rotating weak link. *Phys. Rev. A* , 91, (2015) 033607
18. D. Yan, R. Carretero-González, D. J. Frantzeskakis, P. G. Kevrekidis, Exploring vortex dynamics in the presence of dissipation: Analytical and numerical results.
19. Samson E. C., Wilson K. E., Newman Z. L. and Anderson B. P., Deterministic creation, pinning, and manipulation of quantized vortices in a Bose-Einstein condensate. *Phys. Rev. A* , 93 (2016) 023603